On the Role of Rational Surfaces on Transport in Fusion Plasmas

L. García[1], M. A. Pedrosa[2], C. Hidalgo[2], B. A. Carreras[3], R. Balbín[2], A. López-Fraguas[2], V. E. Lynch[3], J. A. Jiménez[2], B. Ph. van Milligen[2], E. Sánchez[2], and the TJ-II team

1) Universidad Carlos III, 28911 Leganés, Madrid, SPAIN
2) Laboratorio Nacional de Fusión por Confinamiento Magnético,
Asociación EURATOM-CIEMAT, 28040 Madrid, SPAIN
3) Oak Ridge National Laboratory, Oak Ridge, Tennessee 37831-8070, U.S.A.

e-mail contact of main author: lgarcia@fis.uc3m.es

Abstract. Experimental evidence of E×B sheared flows linked to rational surfaces has been obtained in the plasma edge region of the TJ-II stellarator. A possible explanation of the flow structure near the rational surface is the nonlinear beating of the magnetic field component of a vacuum field island with a plasma instability. To simulate the main characteristics of the experimental results, we use a resistive interchange model with the rotational transform profile determined by the vacuum magnetic field calculations.

1. Introduction

Transport barriers in toroidal magnetically confined plasmas tend to be linked to regions of unique magnetic topology such as the location of a minimum in the safety factor, rational q surfaces or the boundary between closed and open flux surfaces [1 and references therein]. Recent experimental results have shown the possible influence of low mode number islands in the formation of edge thermal transport barriers [2]. In the absence of E×B sheared flows, fluctuations are expected to show maximum amplitude near the rational surface. This might tend to deteriorate confinement as suggested by the correlation between energy confinement and the presence of low order rational surfaces at the plasma boundary in W7-AS. On the other hand, if the generation of E×B sheared flows were linked to low order rational surfaces, this might be beneficial for transport. Experimental evidence for such a link has been provided by measurements of the plasma potential and ion saturation current in the boundary region of the TJ-II stellarator [3, 4].

In this paper we present experimental evidence of changes in plasma profiles, and in the turbulence characteristics in the proximity of natural resonances in the TJ-II stellarator. A theoretical study of the influence of rational surfaces on turbulence has been simulated, in terms of the rational surface induced anisotropy and radial non-uniformity in the structure of turbulence, for conditions close to those of TJ-II.

2. Rational surfaces and E×B sheared flows in the TJ-II stellarator

Radial profiles and fluctuations of the ion saturation current have been measured in the proximity of the $n = 8/m = 5$ and $n = 4/m = 2$ natural plasma resonant surfaces. This magnetic surfaces are located near the plasma boundary for different magnetic configurations of TJ-II (stellarator of the Heliac type $R = 1.5$ m, $a \leq 0.22$ m, $B_0 \leq 1.2$T, ECR heating - $P_{ECRH} \leq 600$ kW, f = 53.2 GHz -, pulse length of $\Delta t \leq 250$ ms) [5].

The presence of vacuum magnetic field islands at the natural 8/5 and 4/2 rational surfaces, as predicted by vacuum magnetic field calculations, has been detected as a flattening in the edge profiles in the plasma configuration. Fig 1 shows the radial profiles of the ion saturation current and floating potential measured when the 4/2 rational surface was located in plasma edge region and when the plasma edge was free of low order rational surfaces. Fig. 2 shows profiles of the ion saturation current and plasma potential (computed from the floating potential and electron temperature measurements) in the proximity of the 8/5 rational surfaces. Changes in the shear of E×B flows have been observed near the rational surfaces location with values of the shear decorrelation rate $B^{-1} dE_r/dr \approx 10^5$ s^{-1}. Radial electric fields in the range of 10^3 V/m and poloidal phase velocity of fluctuations of about 500 m/s have been measured [3,4]. The auto-correlation time of fluctuations is in the range $\tau \approx$ 3-15 μs, showing a significant radial variation and

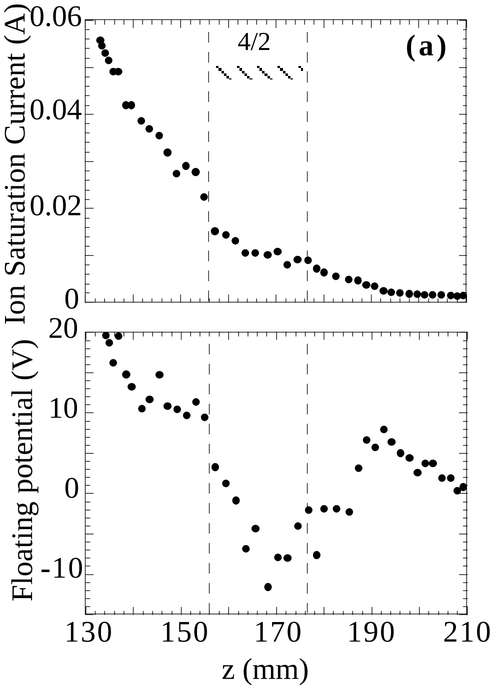

Fig. 1. Radial profiles of the ion saturation current and the floating potential, measured when the 4/2 rational surface was present in the plasma edge region (a) and when it was not (b). The position of the probe (z) is referred to the magnetic axis.

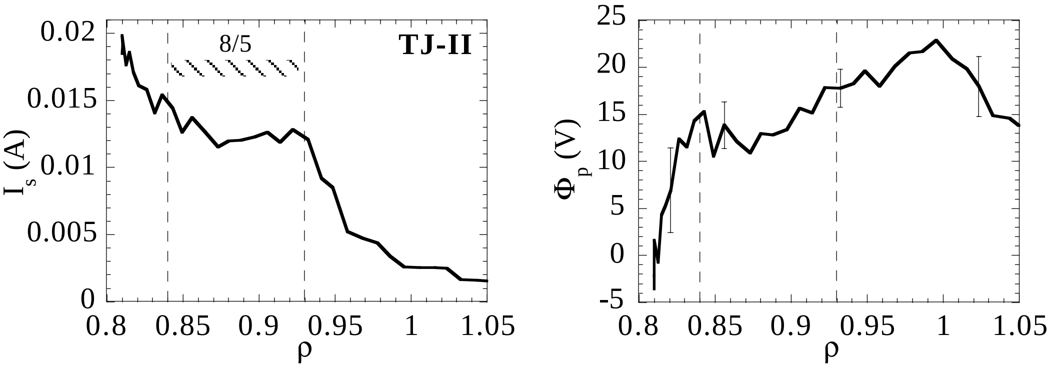

Fig. 2. Radial profile of the ion saturation current (I_s) and plasma potential (Φ_p) in a plasma configuration with a low order resonance located near the plasma boundary.

changes in the proximity of the rational surface location. The resulting E×B decorrelation shearing rate is comparable to $1/\tau$ [3,4].

The poloidal coherence of fluctuations and the coherence between density and poloidal electric field fluctuations show a clear variation in the proximity of the rational surface location. This modification can be explained in terms of the influence of E×B velocity in the cross-correlation of fluctuations measured in the plasma frame of reference and also due to the influence of E×B sheared decorrelation effects [3].

3. Effect of magnetic islands on flow generation and turbulence

A possible explanation of the flow structure near the magnetic island is the coupling of the vacuum magnetic field island with a plasma instability. To study the effect of the magnetic island on flow generation and turbulence, we use a cylindrical-geometry resistive interchange model with the rotational transform profile determined from vacuum magnetic field calculations. The model is based on the reduced MHD equations for the evolution of the poloidal magnetic flux and vorticity plus separated evolution equations for the electron density and temperature. The curvature is determined by the condition that induces the same growth rate as the resistive ballooning mode. The vacuum island is introduced through a non-zero boundary condition for the $n = 8/m = 5$ component of the poloidal flux. The reference plasma parameters are close to those of TJ-II. Since the plasma edge is collisional, we have taken the flow damping rate to be equal to ν_i and we assumed $T_i = T_e = 20$ eV. The simulations are limited to single helicity.

By varying the boundary condition for the $n = 8/m = 5$ component of the poloidal flux, we control the vacuum magnetic field island. In these calculations, we vary ψ_b from $\psi_b = 0$ to $\psi_b = 5\times10^{-4}$, the corresponding width changes from $W = 0$ to $W = 0.09a$. At finite beta, the island width oscillates in time and its averaged value goes from $0.075a$ for $\psi_b = 0$ up to $0.13a$ for $\psi_b = 5\times10^{-4}$. In absence of vacuum magnetic island, there is a poloidal rotation due to the diamagnetic terms. The island associated with the perturbation rotates with a well defined frequency. As ψ_b is increased, the frequency of the perturbation goes through succesive period doublings. At a certain value of ψ_b, the perturbation dynamics reaches chaotic behavior. Above a threshold value of the vacuum magnetic island (below $\psi_b = 2\times10^{-4}$), poloidal propagation stops, and the island evolves again in a quasi-periodic manner.

The poloidal and toroidal averaged density, and temperature at saturation show the flattening caused by the presence of the magnetic island. Another effect of the vacuum magnetic island is the generation of a global poloidal flow through Reynolds stress. The nondiagonal $r\theta$ component of the Reynolds stress tensor has two terms: an electrostatic and a magnetic component,

$$S_{r\theta} \equiv \left\langle \tilde{V}_r \tilde{V}_\theta \right\rangle - \frac{1}{\rho_m \mu_0} \left\langle \tilde{B}_r \tilde{B}_\theta \right\rangle .$$

Below the threshold, the electrostatic and magnetic components of the Reynolds stress have similar size and radial profiles, but the opposite sign (Fig 3a). This causes a near cancellation of these two terms, as it happens in the case of electromagnetic turbulence [6, 7]. In this situation, the electrostatic component is slightly larger than the magnetic. Above the threshold, the vacuum magnetic island induces a non-negligible contribution to the magnetic component making the latter dominant (Fig. 3b), and a strong sheared flow is established. This shear flow has generally the opposite sign than the one below the threshold.

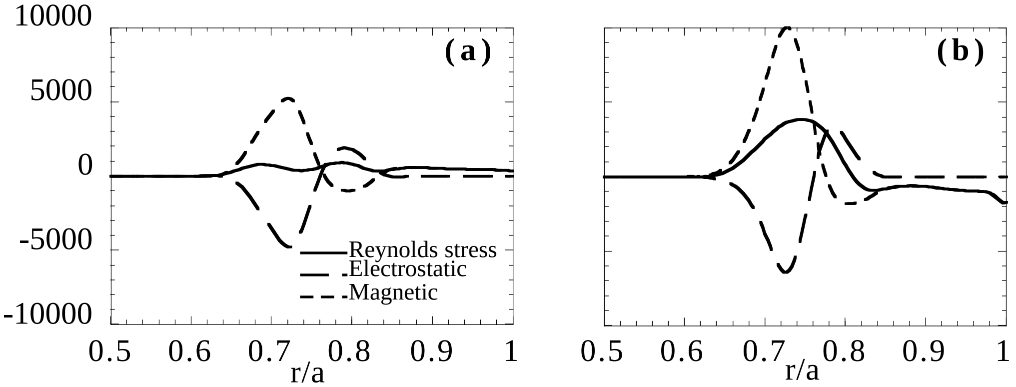

Fig. 3. Radial profiles of the Reynolds stress and its components for $\psi_b = 5\times10^{-5}$ (a), and $\psi_b = 2\times10^{-4}$ (b). They are obtained by averaging in the saturation phase.

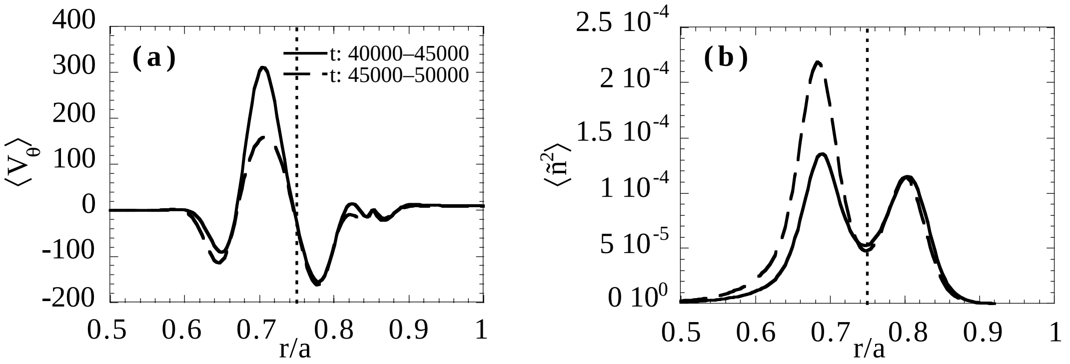

Fig. 4. Radial profiles of the poloidal flow (a), and r.m.s. value of the density fluctuation (b) for $\psi_b = 10^{-4}$*. They are obtained by averaging in two different time intervals in the saturation phase.*

The poloidal flow oscillates in time and changes direction in a quasiperiodic manner. The averaged poloidal flow has radial spikes just outside the magnetic island and causes a reduction in the plasma turbulence level. This can be seen in Fig. 4, where the averaged poloidal flow, and the r.m.s. value of the density fluctuation are plotted as a function of radius. The profiles are obtained by averaging in time in two different time intervals in the saturation phase. In consistency with TJ-II experiments, results show the generation of shear, and a reduction of fluctuations close to the position of the island associated with the resonant surface. It is apparent from the figure that the fluctuation level is linked to the shear in the poloidal flow. The level of generated shear flow at the rational surface increases with the vacuum magnetic island width and, at a critical value of the island width, it reverses sign and becomes very large.

However, the saturation level of the fluctuations is only slightly decreased for island widths below the threshold, and, in spite of the strong sheared flow, the fluctuation level increases for island widths above the threshold (Fig. 5a). The turbulent flux remains almost the same as the vacuum magnetic island increases (Fig. 5b). We use the following form for the calculation of the flux:

$$\Gamma_{\text{model}} = \overline{\left\langle \left(V_r - \langle V_r \rangle\right)\left(n - \langle n \rangle\right) \right\rangle}, \tag{1}$$

where the upper bar indicates time-average, and the angular brackets, $\langle\ \rangle$, indicate average over the flux surface. In the experiment, with data measured at a single poloidal location, the flux is often calculated as

$$\Gamma_{\text{exp}} = \overline{\left(V_r - \overline{V}_r\right)\left(n - \overline{n}\right)}. \tag{2}$$

In absence of vacuum magnetic island and with poloidal propagation of the turbulence, both results are similar, and the experimentally calculated flux at any of the poloidal positions gives a good estimate of the real averaged flux within a factor of 2. The situation changes totally when poloidal propagation of some or all fluctuation components stops. Eq. (2) underestimates the flux practically in all positions, and even results in a strong negative flux in some poloidal positions, because the estimates of the averaged fluctuation level is erroneous and close to its local value.

Similar results were obtained in the study of resistive pressure-gradient-driven turbulence with an external sheared flow [7]. In that case, the numerical results showed that shear flow effects were not significant when the single helicity dominated near the low-*m* rational surfaces. Therefore, multiple helicity calculations are needed to assess the effect of vacuum islands on turbulence. These calculations are now underway.

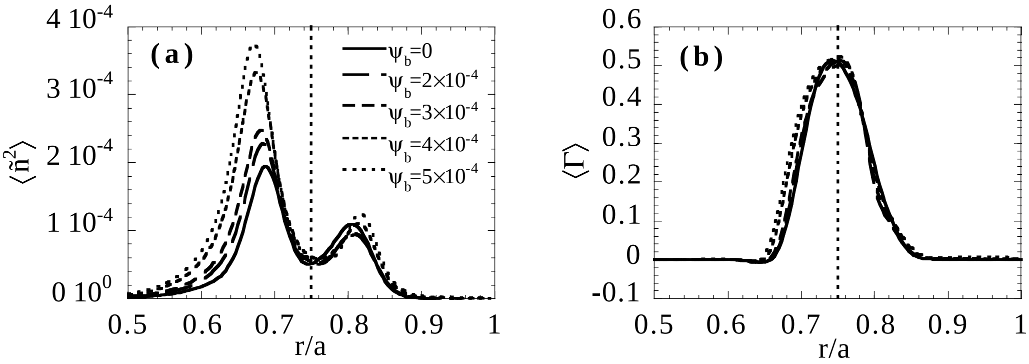

Fig. 5. Radial profiles of the r.m.s. value of the density fluctauation (a), and the particle flux (b) for different sizes of the vacuum magnetic island. They are obtained by averaging in the saturation phase.

4. Conclusions

Experiments in the TJ-II stellarator show the formation of ExB sheared flows in the proximity of rational surfaces. These results can be interpreted in terms of the symmetry-breaking mechanisms in the radial-poloidal structure of fluctuations (i.e. Reynolds stress) at rational surfaces. We have used a resistive interchange model to study the effect of magnetic islands on poloidal flow generation and turbulence. For vacuum magnetic islands below a threshold value, there is a near cancellation of the electrostatic and magnetic components of the Reynolds stress. Above the threshold, the magnetic component dominates and a strong sheared flow is established. In spite of that, the fluctuation level increases, and the flux remains almost the same.

Care should be taken when evaluating the turbulent flux in stellarators. The presence of small vacuum magnetic field islands can stop the poloidal propagation of some of the fluctuation components. In this case, the flux surface average and time average are not equivalent. This may result in an erroneous estimation of the averaged value of the fluctuations and as a consequence of the fluxes.

Acknowledgments

This research is sponsored by the Dirección General de Enseñanza Superior (Spain) under Project No. PB96-0112-C02. Part of this research has been carried out at Oak Ridge National Laboratory, managed by UT-Battelle, LLC, for the U.S. Department of Energy under contract number DE-AC05-00OR22725.

References

[1] SYNAKOWSKI, E., Plasma Phys. Control. Fusion **40** (1998) 581.
[3] OHYABU, K., et al., Phys. Rev. Lett. **84** (2000), 103.
[3] PEDROSA, M. A., et al., Proc. 27th EPS Conference on Controlled Fusion and Plasma Physics, Budapest, 2000.
[4] HIDALGO, C., et al., Plasma Phys. Control. Fusion **42** (2000) A153.
[5] ALEJALDRE, C., et al., Plasma Phys. Control. Fusion **41** (1999) B109.
[6] CRADDOCK, G. G., DIAMOND, P. H., Phys. Rev. Lett. **67** (1991) 1535.
[7] CARRERAS, B. A., et al., Phys. Fluids B **5** (1993) 1491.